

Simultaneous determination of sunset yellow and tartrazine in soft drinks samples using nanocrystallites of spinel ferrite-modified electrode

Masoumeh Taei^a, Hossein Salavati^{a,*}, Masoud Fouladgar^b, Elmira Abbaszadeh^a

^aDepartment of Chemistry, Payame Noor University, 19395-4697 Tehran, Iran

^bDepartment of Chemistry and Biochemistry, Falavarjan Branch, Islamic Azad University, Isfaham, Iran

Received: 2 May 2019, Accepted: 4 August 2019, Published: 1 January 2020

Abstract

The ZnCrFeO₄ nanoparticles were synthesized as antiferromagnetic material using sol-gel method. The X-ray diffraction (XRD) analysis and transmission electron microscopy (TEM) certified that ZnCrFeO₄ nanoparticles have single-phase cubic structure with a range of 50–100 nm in size. A facile and sensitive analytical method was developed for simultaneous determination of sunset yellow and tartrazine based on ZnCrFeO₄ modified paste electrode. The oxidation responses of sunset yellow and tartrazine are improved extremely at the modified carbon paste electrode (ZnCrFeO₄/CPE), exhibiting two well-defined anodic peaks at +0.70V and +0.99 V vs Ag/AgCl, respectively. The oxidation reactions were controlled by diffusion step for tartrazine and adsorption step for sunset yellow. Simultaneous determination of these dyes indicated wide linear ranges from 0.07 to 47.5, and 0.05 to 19.0 μmol L⁻¹ with detection limits of 2.0 and 10.0 nmol L⁻¹ for sunset yellow and tartrazine, respectively. The results of real samples analyses affirmed that ZnCrFeO₄/CPE possess remarkable potential to determine simultaneously sunset yellow and tartrazine in soft drinks samples.

Keywords: Modified carbon paste electrode; sunset yellow and tartrazine; sol-gel method; ZnCrFeO₄.

Introduction

Sunset yellow (SY) and tartrazine (TZ) are synthetic azo colorants, which can be found in some food products such as candies, beverages, prawn slices and dairy products [1]. The concentration level of these dyes must be checked due to having mutagenic and carcinogenic effects on human beings. For instance, TZ shows various allergic reactions and

side effects, which contain eczema, migraines, anxiety, blurred vision, asthma attacks, other skin rashes, eosinophilia thyroid cancer, and clinical depression [2,3]. Although it seems that side effects of SY are less than TZ, SY also causes a number of side effects (headache, sinus attacks, constipation, blood pressure and sleeping disorders) and allergies in some people. Recent

*Corresponding author: Hossein Salavati

Tel: +98 (31) 33521804, Fax: +98 (31) 33521802

E-mail: hosseinsalavati@pnu.ac.ir

studies show that different analytical methods have been utilized to determine these synthetic colors in food products such as spectrophotometry [4], liquid chromatography [5], fluorometry [6], and electrochemistry [7]. However, electrochemical methods have received so much attention because of sensitivity, cheapness and fast responses. In addition, determination of SY and TZ in food products with spectroscopic methods needs separation technique as sample handling and preparation.

Recently, application of nanomaterials has been considered in various fields including, electrochemistry [8,9], nuclear energy [10], pollutants removal [11], etc.

Normal spinel with general formula $A^{2+}B_2^{3+}O_4^{2-}$ revealed a class of materials, having A^{2+} and B^{3+} in the octahedral and tetrahedral sites [12]. Having unique electrical and magnetic properties, nanosized spinel ferrites have been used in diverse fields such as high-density data storage, ferrofluid technology, sensor construction, spintronics, drug delivery, magnetocaloric refrigeration, magnetic resonance imaging, and heterogeneous catalysis [13]. In sensor technology, spinel ferrites such as Fe_3O_4 , $NiFe_2O_4$, $MgCrFeO_4$, $CoFe_2O_4$, and $ZnFe_2O_4$ have been applied as novel electrocatalytic modifiers. A simple fabricated device for determination of hydrogen peroxide was reported by utilizing $ZnFe_2O_4$ /chitosan modified gold electrode in serum samples [14]. A sensitive and rapid voltammetric sensor towards simultaneous determination of codeine and oxycodone was used based on $CoFe_2O_4$ nanoparticles modified carbon paste electrode [15]. A glassy carbon electrode modified with Pt/Fe_3O_4 /reduced-graphene oxide was investigated for electrocatalytic

oxidation of NADH (nicotinamide adenine dinucleotide hydride) [16]. A meritorious mention would be the development of multi-walled carbon nanotubes decorated with synthesized $NiFe_2O_4$ magnetic nanoparticles for the voltammetric determination of cefixime [17]. A highly selective electrochemical sensor towards determination of phenazopyridine was constructed based on $MgCr_2O_4$ nanoparticles decorated multi-walled carbon nanotubes-modified glassy carbon electrode [18]. Chemical modification of carbon paste electrode (CPE), having renewal surface, has been widely reported [19]. The carbon paste electrode with novel modifiers provides us with a wider diversity of sensors to determine species environmentally and biologically.

The purpose of the present work is to fabricate a sensitive and simple voltammetric sensor for simultaneous detection of SY and TZ with upgraded detection limit free from the effects of possibly interfering species. The carbon paste electrode was modified by $ZnCrFeO_4$ nanoparticles and electrochemical behaviors of SY and TZ explained by cyclic voltammetry (CV) on modified electrode. The oxidation signals of SY and TZ at $ZnCrFeO_4$ /CPE were compared to that at pure carbon paste electrode (CPE). The fabricated electrode was applied to determine SY and TZ individually and simultaneously. The obtained results are extremely prosperous, therefore, $ZnCrFeO_4$ modified carbon paste electrode is a qualified sensor for the selective determination of SY and TZ with practical utility.

Experimental

Apparatus and chemicals

The Metrohm instrument Model 797 VA, which is coupled with a conventional three-electrode cell was

utilized for all voltammetric measurement. The ZnCrFeO₄/CPE, Ag/AgCl electrode (Azar Electrode, Iran), and a platinum wire were used as working electrode (Azar Electrode, Iran), reference electrode and counter electrode, respectively. For pH adjustment, a Metrohm model 691 pH/mV meter was utilized. XRD (X-ray diffraction analysis) (Holland Philips Xpert, X-ray diffractometer with Cu-K_α radiation) and FE-SEM (Field Emission Scanning Electron Microscopy) (Hitachi S-4160) were used to clarify the structure and morphology of magnetic nanoparticle. Fourier transformed infrared (FT-IR) spectra of spinel in a pressed KBr matrix was conducted with a FT-IR, Jasco 4200 spectrometer in the range 4000-400 cm⁻¹.

All the chemicals with analytical grade purity were used. SY and TZ were purchased from Aldrich, and dissolved into water to prepare 1.0×10⁻³ mol L⁻¹ standard solutions. 0.10 mol L⁻¹ phosphate buffer solutions in the pH range of 3- 8 values were applied.

Synthesis procedure for ZnCrFeO₄ nanoparticles

The ZnCrFeO₄ nanoparticles were synthesized according to previous reported method [20]. In this method, 8.07 g of Fe(NO₃)₃.9H₂O, 5.94 g of Zn(NO₃)₂.6H₂O and 8.00 g of Cr(NO₃)₃.9H₂O were transferred to a 100 mL round bottom flask. Then, 50 mL methanol as solvent was added and then a solution containing ammonium hydroxide was added to this mixture until the pH = 9 was achieved. The obtained sample was stirred at 80 °C for 20 min. After that, stirring was carried out for one day. The product was rinsed with double distilled water several times and then permitted to dry at 60 °C. Finally, the nanoparticles

were prepared by heating in electric furnace for 120 minutes at 900 °C.

Preparation of ZnCrFeO₄ modified electrode

To fabricate the ZnCrFeO₄ spinel modified electrode, a mixture of 0.05 g of ZnCrFeO₄, 0.20 g of graphite, and 10 mL diethyl ether were sonicated to form uniform black solid phase after ether evaporation. Then, 50 mg paraffin was added to prepare ZnCrFeO₄ carbon paste. The obtained paste was inserted in a glass tube. The electrical connection was executed by a copper wire, which was installed into another head of the glass tube. The pure carbon paste electrode (CPE), utilized for comparison, was constructed in the same way, however, the nanoparticles addition stage was omitted. The anodic response of SY and TZ was studied at CPE and ZnCrFeO₄/CPE by CV and DPV (differential pulse voltammetry) under optimized conditions.

Results and discussion

Morphological characterization of ZnCrFeO₄ nanoparticles

The phase purity and crystal structure of the ZnCrFeO₄ nanoparticles have been studied by XRD. Figure 1A illustrates characteristic peaks that occur at 2θ of 30.08, 35.36, 37.08, 43.08, 53.27, 56.93 and 62.44 that are signed by their corresponding crystallographic planes (220), (311), (222), (400), (422), (511) and (440), respectively. The XRD results completely certified that ZnCrFeO₄ (Cubic, JCPDS no. 430554) was produced. In addition, XRD patterns shows absence of any impurities in prepared sample. D parameter, which is defined as crystallite size of the ZnCrFeO₄ sample, was calculated according to Scherer's equation:

$$D = 0.9\lambda/\beta \cos\theta$$

In the mentioned formula, λ and β refer to the wavelength of X-ray and full width at half maximum of the peak at diffracting angle θ , respectively. The D of the prepared ZnCrFeO₄ nanoparticles was easily obtained about 3.0 nm. The structure of ZnCrFeO₄ nanoparticle was investigated using the fourier transform infrared (FT-IR) spectroscopy analysis and this study entirely affirmed the synthesis of spinel structure. There are three identified peaks in FT-IR pattern related Fe³⁺-O²⁻

, Zn²⁺-O²⁻ and Cr³⁺-O²⁻ which are located at 410, 615 and 490 cm⁻¹, respectively. The FT-IR analysis of prepared sample coincides with previously reported works [21,22].

Figure 1B indicates that ZnCrFeO₄ nanoparticles with spherical shape agglomerated and the mean size diameters of particles using Digimizer (as image analysis software) is in the range of 50-100 nm.

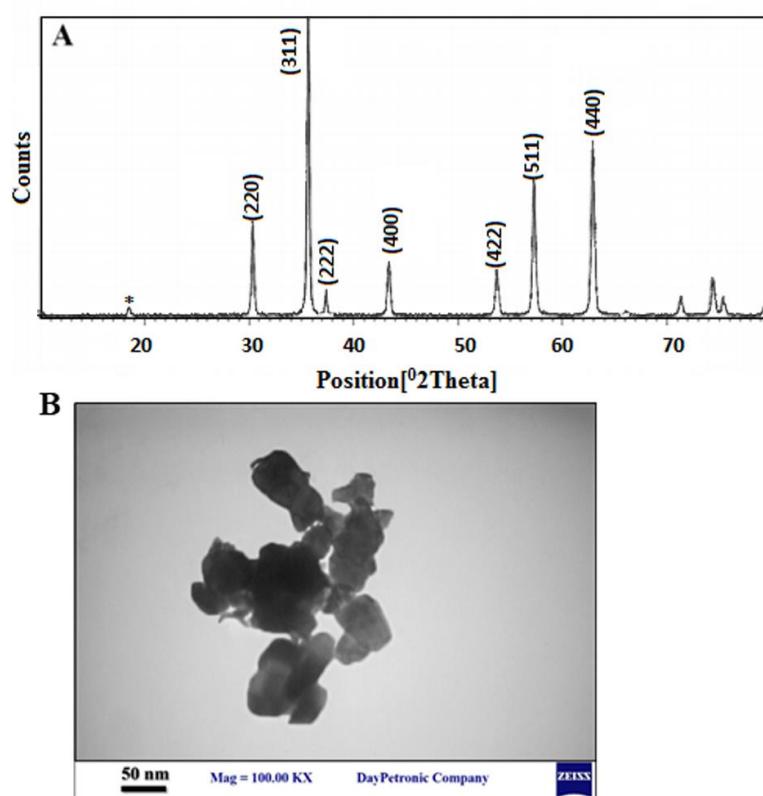


Figure 1. XRD patterns (A) and TEM (B) of the synthesized ZnCrFeO₄ nanoparticles

Calculation of the effective surface area of ZnCrFeO₄ modified electrode

The electroactive surface areas of the pure CPE and ZnCrFeO₄/CPE were appraised by CV technique in the range of 0.0 to 0.6 V for 1.0 mM K₃Fe(CN)₆ as a probe in 0.1 M KCl. The slope of I_p vs. $v^{1/2}$ curve was determined by varying scan rate from 0.01 to 0.15 V/s and the electroactive surface area was

obtained from the Randles-Sevcik equation for a reversible process [23].

$$I_{pa} = 2.69 \times 10^5 n^{3/2} A C_0 D_R^{1/2} v^{1/2}$$

Where I_{pa} denotes to the anodic peak current (A), n presents the electron number, A refers to the surface area of the electrode (cm²), D_R defines diffusion coefficient (cm²s⁻¹), C_0 shows the concentration of K₃Fe(CN)₆ and v is the scan rate Vs⁻¹. At temperature of 298 K, $n=1$, $F=96480$ C mol⁻¹, and D_0

$= 7.6 \times 10^{-6} \text{ cm}^2 \text{ s}^{-1}$, the active electrode surfaces area were 0.389 cm^2 for the CPE, and 0.761 cm^2 for ZnCrFeO_4 modified electrode, which is approximately 2.0 times greater than that for pure CPE.

Morphological characterization of $\text{ZnCrFeO}_4/\text{CPE}$

The FE-SEM micrographs of CPE and $\text{ZnCrFeO}_4/\text{CPE}$ were analyzed to identify their own characteristics. Figure 2A illustrates that CPE is composed of crumpled sheets associated with each other. In

comparison to bare CPE, spinel ferrites nanoparticles completely have filled pores and size of cavities in the matrix of CPE (Figure 2B). In fact, the real surface area was increased obviously at $\text{ZnCrFeO}_4/\text{CPE}$. Figure 2B also reveals that nanoparticles have spherical shape which uniformly dispersed at the matrix. In addition, EDX analysis exactly shows the presence of Zn, Fe, Cr, and O elements in ZnCrFeO_4 paste (Figure 2C).

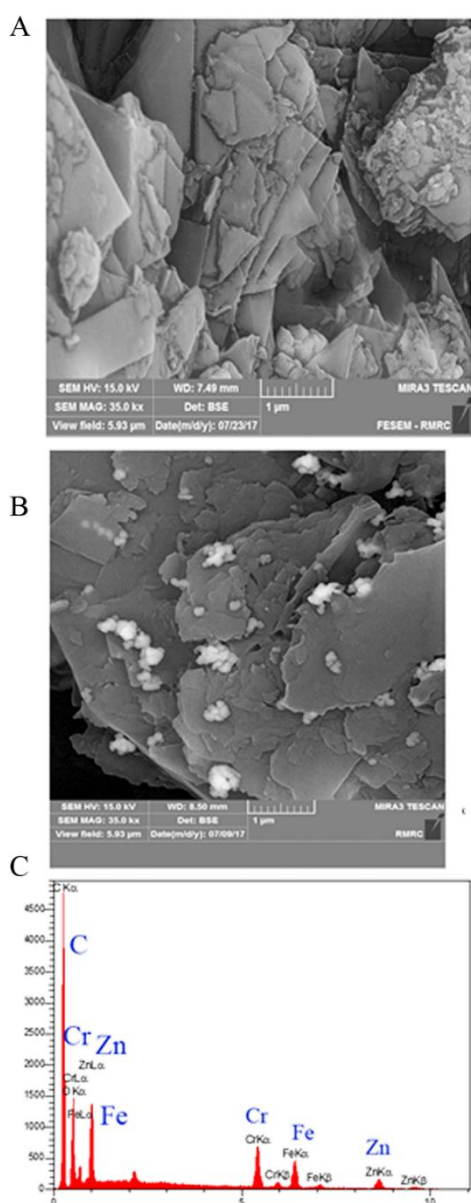


Figure 2. FE-SEM image of: (A) CPE, (B) ZnCrFeO₄/CPE, (C) the corresponding EDX spectrum taken from the whole area of (B)

Electrochemical impedance spectroscopy (EIS) was applied to analyze the electronic conductivity changes at surface of chemically modified electrodes [23]. The Nyquist diagram containing a semicircle diameter at high frequencies, which shows the electron-transfer resistance (R_{ct}), and a linear portion at low frequencies might be appoints to diffusion process [23]. Figure 3 shows the Nyquist plots of the bare CPE (a),

and ZnCrFeO₄/CPE (b). The equivalent circuit shown in Figure 3 containing the circuit consists of R_s as solution resistance, W is Warburg impedance, Q appoints to the constant phase element, and R_{ct} refers to the charge transfer resistance [23]. The R_{ct} value of ZnCrFeO₄/CPE decreased remarkably (about 448 Ω), that attributed to the supreme conducting properties of the ZnCrFeO₄ through facilitation electron transfer and increase surface area.

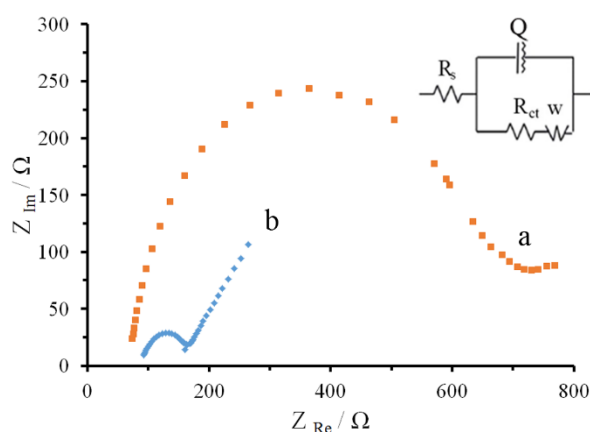


Figure 3. Impedance spectra of (a) CPE, (b) ZnCrFeO₄/CPE, in 3.0 mmol L⁻¹[Fe(CN)₆]^{3-/4-} containing 0.1 mol L⁻¹ KNO₃. Conditions: polarization potential: 0.15 V, frequency: 5.0 × 10⁻³ to 10⁵ Hz.

Electrochemical behavior of SY and TZ at the surface of modified electrode

Figure 4 shows the cyclic voltammograms (CVs) of 2.0 $\mu\text{mol L}^{-1}$ of SY and 7.0 $\mu\text{mol L}^{-1}$ of TZ at bare CPE (curve a) and ZnCrFeO₄/CPE (curve b). Bare CPE exhibits two anodic peaks at +0.70 V and +0.99 V for SY and TZ, respectively. At modified electrode, there are intensified anodic peaks at the same potentials, offering that ZnCrFeO₄ nanoparticles are effective to improve the electrochemical behavior of SY and

TZ. The fabricated sensor amplifies the anodic current of analytes. In fact, the ZnCrFeO₄/CPE caused about 2.0-fold increase in oxidation peaks of two components. This behavior is due to increasing active surface area of electrode and also fascinating electron transfer. Moreover, the higher background current at ZnCrFeO₄/CPE also certified that the real surface area of modified electrode has been increased.

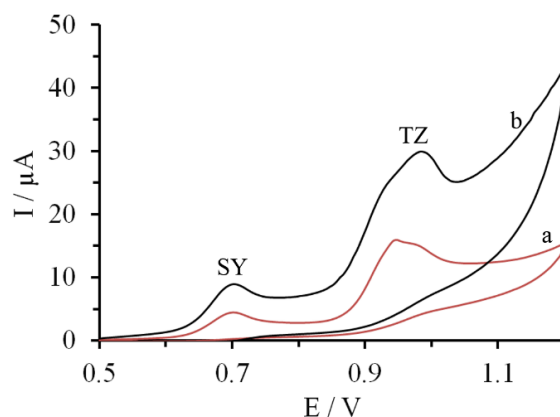


Figure 4. Cyclic voltammograms of $2.0 \mu\text{mol L}^{-1}$ of SY and $7.0 \mu\text{mol L}^{-1}$ of TZ at (a) CPE, (b) $\text{ZnCrFeO}_4/\text{CPE}$. sweep rate: 50 mV s^{-1} ; phosphate buffer (0.1 mol L^{-1} , pH 6.0)

The kinetics of oxidation reactions at $\text{ZnCrFeO}_4/\text{CPE}$ were examined and the effects of scan rate on the anodic signals of SY and TZ were studied. Figure 5 presents changes in cyclic voltammograms of SY (A) and TZ (B) by varying scan rates. It is crystal clear that SY shows a reversible behavior, while TZ indicates an irreversible peak at the surface of modified electrode. In addition, the

oxidation currents of SY and TZ increased linearly with v and $v^{1/2}$, respectively. In fact, the oxidation reaction rate was controlled by a diffusion step for TZ, while it is an adsorption reaction for SY. In fact, the adsorption of SY caused a preconcentration at the surface of modified electrode, and subsequently improved the detection limit.

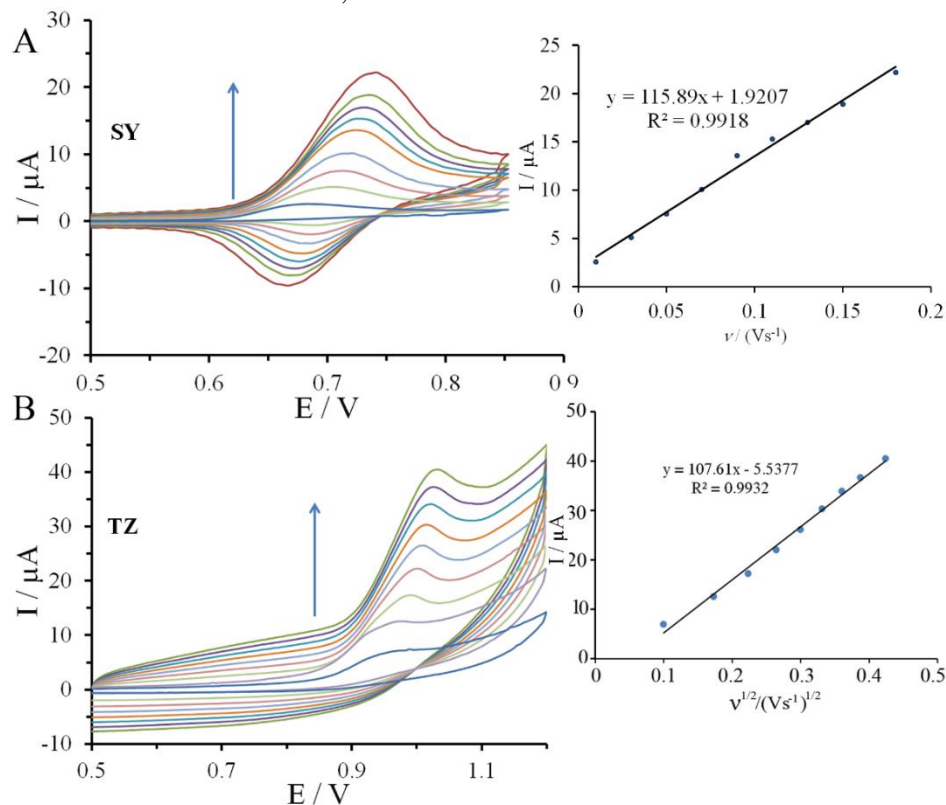
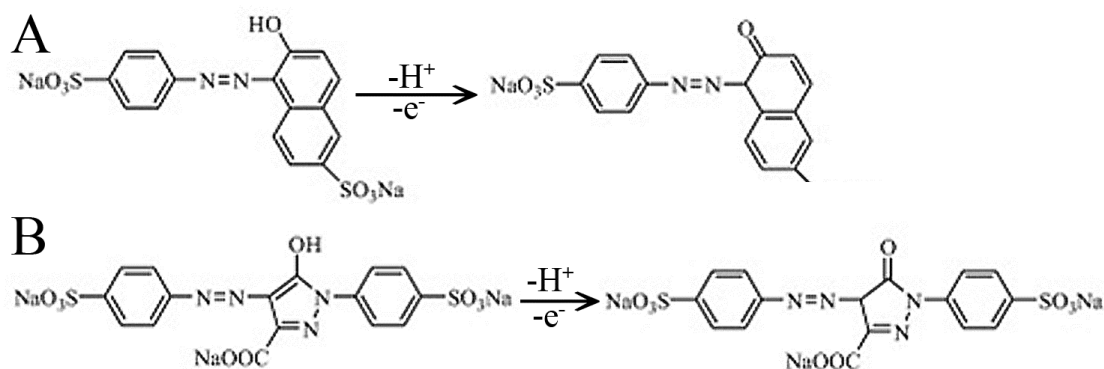


Figure 5. Cyclic voltammograms of (A) $50.0 \mu\text{mol L}^{-1}$ SY and (B) $100.0 \mu\text{mol L}^{-1}$ TZ at $\text{ZnCrFeO}_4/\text{CPE}$ with various scan rates at pH=6.0



Scheme 1. Electro-oxidation mechanism of A) SY and B) TZ

The influence of pH on electrochemical behaviors of $30.0 \mu\text{mol L}^{-1}$ of SY and $100.0 \mu\text{mol L}^{-1}$ of TZ at $\text{ZnCrFeO}_4/\text{CPE}$ was investigated by DPV method. The best anodic response of modified electrode for SY and TZ was achieved in the pH range 3.0 to 6.0. However, the oxidation currents of both SY and TZ decreased at alkaline (pH > 8) condition. In fact, these dyes convert to anion forms at basic medium and an electrostatic repulsion between analytes and modifier may cause a significant decrease in oxidation signals of two dyes. Literatures showed that electrochemically oxidation of SY and TZ contains proton exchange [24], which is exactly similar to what happened at the surface of the proposed electrode (Scheme 1). In fact, the peak potential of two compounds shifted to negative values at higher pH values. Regarding the selectivity and sensitivity of the fabricated sensor, pH 6.0 was favorable as the optimal experimental condition.

Electrochemical determination of SY and TZ

For individual determinations, the typical differential pulse voltammograms of SY and TZ were displayed in Figure 6. Optimized differential pulse parameters were used

for this purpose including 100.0 ms pulse interval, 40.0 ms pulse width, and 50.0 mV pulse amplitude. The linear oxidation responses of SY and TZ were in the concentration ranges of 0.07 to 47.5 and 0.05 to 19.0 $\mu\text{mol L}^{-1}$, respectively. The detection limits of 0.02 and 0.01 $\mu\text{mol L}^{-1}$ according to $S/N = 3$ were obtained for SY and TZ, respectively. Figure 7A reveals that the oxidation peak currents of SY linearly proportioned with the concentration level of SY in the solution, and the presence of 15.0 $\mu\text{mol L}^{-1}$ TZ has negligible change when the concentration of SY has been increased. This Linear relation between concentration of SY and signal current can be expressed by the following equation: $I_{pa} (\mu\text{A}) = 0.1165 C (\mu\text{mol L}^{-1}) + 0.4903$ ($R = 0.9931$). Similarly, Figure 7B illustrated the DPV curves of TZ containing 6.0 $\mu\text{mol L}^{-1}$ SY. Similarly, when the concentration level of TZ was increased, no obvious change was observed in anodic peak of SY. The linear concentration range for individual determination of TZ was from 0.05 to 19.0 $\mu\text{mol L}^{-1}$ with a linear equation of $I_{pa} (\mu\text{A}) = 0.161 C_{TZ} (\mu\text{mol L}^{-1}) - 0.0195$ ($R = 0.9934$).

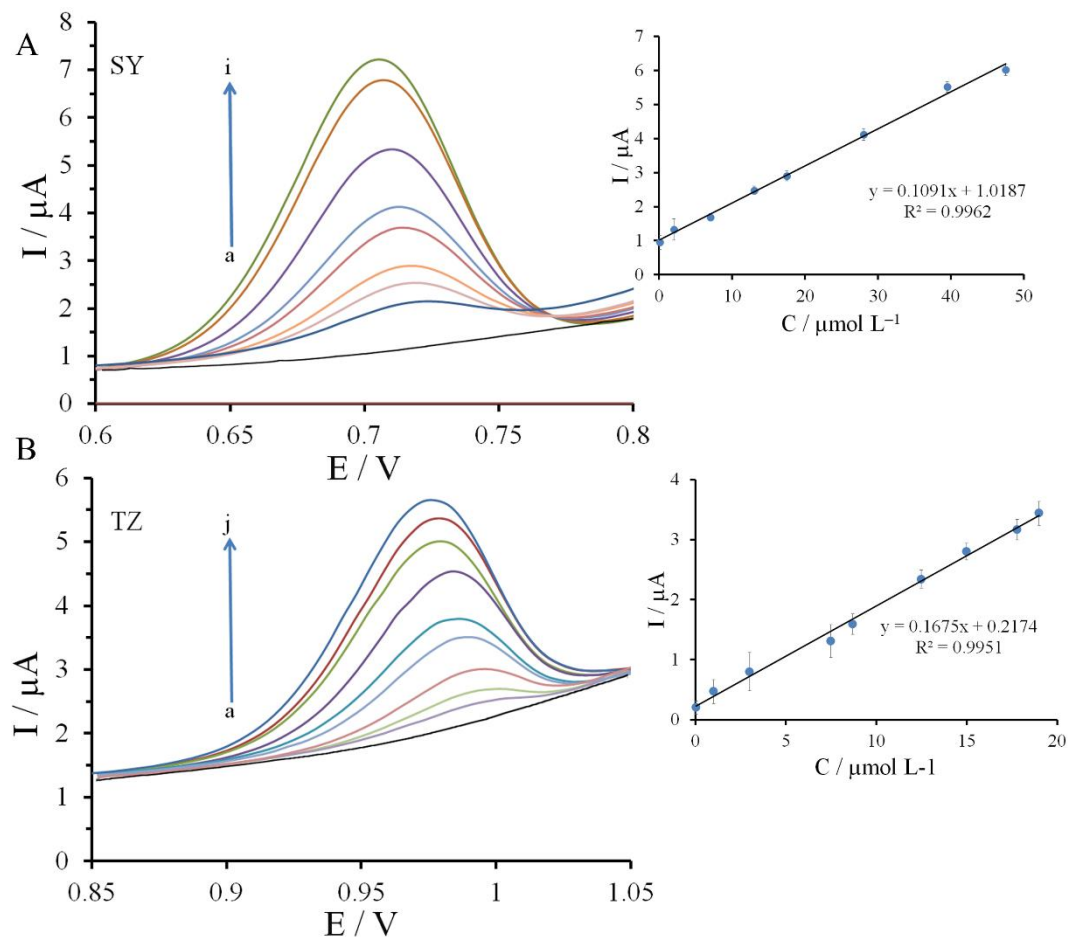


Figure 6. A) DPV of ZnCrFeO₄/CPE in a) 0.0; b) 0.07; c) 2.0; d) 7.0; e) 13.0; f) 17.5 ;g) 28.0; h) 39.5; and i) 47.5; μmol L⁻¹ SY, B) DPV of ZnCrFeO₄/CPE in a) 0.0; b) 0.05; c) 1.0; d) 3.0; e) 7.5; f) 8.7; g) 12.5.; h) 15.0; i) 17.8;and j) 19.0 μmol L⁻¹ TZ at pH 6.0

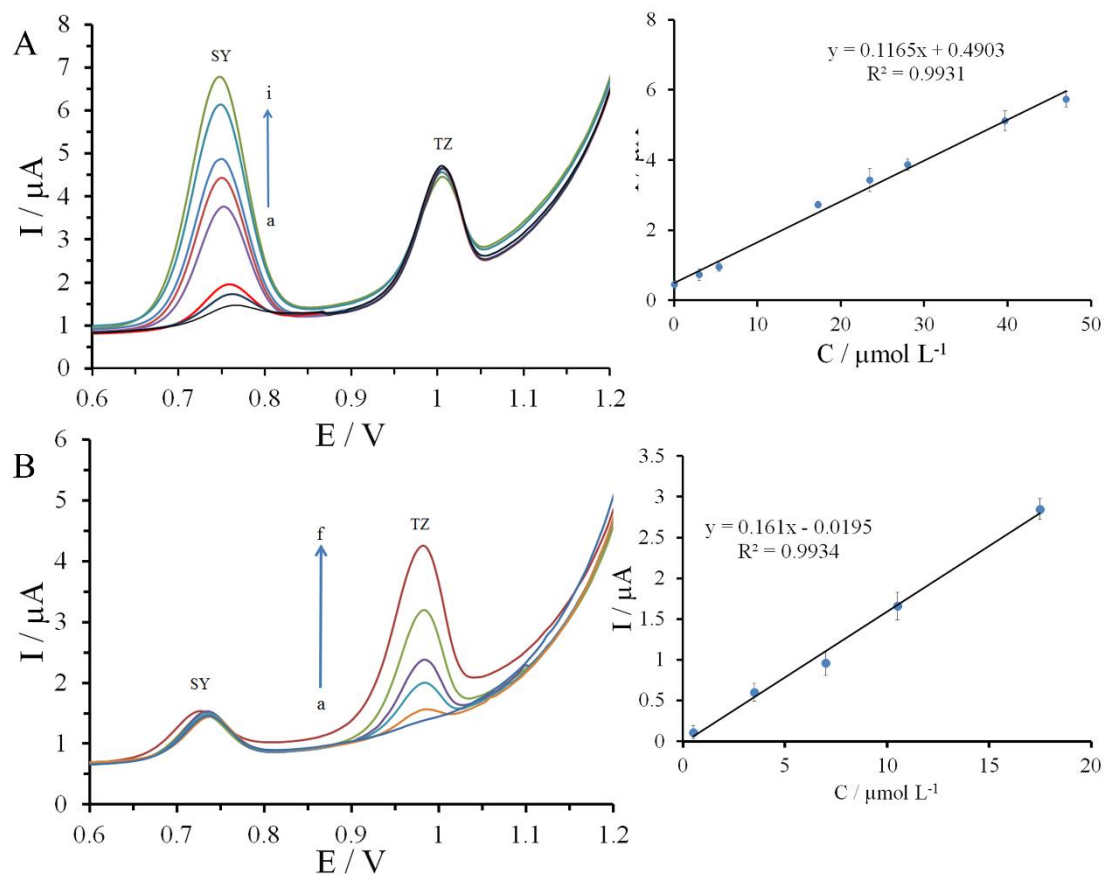


Figure 7. A) DPV of $\text{ZnCrFeO}_4/\text{CPE}$ in (a) 0.0; (b) 0.1; (c) 3.0; (d) 5.4; (e) 17.3; (f) 23.5; (g) 28.0 (h) 39.7, and (i) $47.0 \mu\text{mol L}^{-1}$ SY, in the presence of $19.0 \mu\text{mol L}^{-1}$ TZ at pH 6.0. B) DPV graphs of $\text{ZnCrFeO}_4/\text{CPE}$ in (a) 0.0; (b) 0.5; (c) 3.5; (d) 7.0; (e) 10.5; and (f) $17.5 \mu\text{mol L}^{-1}$ TZ in the presence of $70.0 \mu\text{mol L}^{-1}$ SY

The analytical parameters were compared with the reported voltammetric sensors, which are listed in Table 1 [24-29]. It is inferred that our method possess lower detection limits for simultaneously determination of SY and TZ than other reported works. The F (Fisher-Snedecor) and then Student's t-tests utilized to verify the sensitivities of method for two compounds in the absence and presence of each other were the same. The estimated values of F and t-tests were less than that of theoretical F and t values (at the 95% of the confidence level,) indicating that there is no considerable difference between the calibration slopes of SY and TZ in the two states. This fact completely certified that two mentioned dyes did not interfere in the measurement of each other.

The reproducibility of the $\text{ZnCrFeO}_4/\text{CPE}$ was searched for a solution containing $5.0 \mu\text{mol L}^{-1}$ of SY and TZ, the relative standard deviations (RSDs) of the oxidation signals at six independently constructed ZnCrFeO_4 modified electrodes were 3.47% and 3.65%, respectively, indicating passable reproducibility. The stability of $\text{ZnCrFeO}_4/\text{CPE}$ was tested every week for 2 months a solution containing $5.0 \mu\text{mol L}^{-1}$ of SY and TZ. The low values of RSDs (less than 5%) affirmed that the electrode preserved more than 95% of its ability for simultaneous determination of these organic dyes. Furthermore, the overall repeatability (RSD) of the $\text{ZnCrFeO}_4/\text{CPE}$ for $5.0 \mu\text{mol L}^{-1}$ of SY and TZ for three recorded DP voltammograms were 2.1% and 3.7% respectively.

Table 1. Comparison of some characteristics of the different modified electrodes for the determination of SY and TZ

Working electrode	Limit of detection (nmol L ⁻¹)		Linear dynamic range(μmol L ⁻¹)		References
	SY	TZ	SY	TZ	
MWNT/GCE	22.0	188.0	0.0553–110.0	0.374–748.0	[1]
ZnO/Cysteic acid/GCE	30.0	10.0	0.1–3.0	0.07–1.86	[24]
Au NPs/CPE	30.0	2.0	0.1–2.0	0.05–1.6	[25]
GN-PTA/GCE	1.1	56.1	0.0332–0.464	0.112–2.81	[26]
MWCNTs-IL/CCE	100.0	1100.0	0.4–110	3.0–70.0	[27]
GN/TiO ₂ /CPE	6.0	8.0	0.02–2.05	0.02–1.18	[28]
Hanging mercury drop electrode	11.0	-	0.011–0.2	-	[29]
ZnCrFeO ₄ paste electrode	2.0	10.0	0.07–47.5	0.05–19.0	This work

Interference study

The possible interferences of some substrates such as coloring agents, inorganic ions, sweeteners, and preservatives might be co-existed in real samples which were studied toward detection of SY and TZ. It was found that 500-fold of the following interferences including vitamin C, glucose, and sucrose 300-fold concentration of sodium citrate, and sodium oxalate did not change the oxidation signal of SY and TZ significantly. The effects of some inorganic ions mostly found in food products were also investigated in detection of these synthetic azo dyes. The results reveal that 500-fold concentration of Mg²⁺, Cl⁻, Na⁺, Fe³⁺, K⁺, Fe²⁺, and SO₄²⁻ did not observed any considerable change in oxidation signals. In addition, other materials such as uric acid, L-cysteine, L-tyrosine, L-serine, L-glutamine, and valine caused changes in main signals of SY and TZ lower than 5%. As a result, the proposed electrode was extremely selective toward detection of SY and TZ in complex matrices.

Determination of SY and TZ in beverage samples

To evaluate the reliability and practical applicability of ZnCrFeO₄/CPE for simultaneous determination of SY and TZ, two famous brands of soft drinks Fanta, and Mirinda, were selected. For these analyses, no special preparation was essential. After suitable dilution with supporting electrolyte pH=6.0, the potential was scanned from 0.4 to 1.2 V, two distinctive peaks were observed corresponding to SY and TZ oxidation signals, indicating the modified electrode can be utilized for practical application. Furthermore, the standard addition method was exerted to determine the exact content of SY and TZ in drink samples (Table 2). The satisfying recoveries of the three drinks were in the range of 99.0–102.1% for SY and 98.1–99.0% for TZ, respectively, demonstrating that the proposed sensor could be applied to the individually or simultaneously determination experiments SY and TZ adequately.

Table 2. Simultaneous determination of SY and TZ in drink samples

Sample	Analyte	Added ($\mu\text{mol L}^{-1}$)	Found ($\mu\text{mol L}^{-1}$)	Recovery%
Fanta	SY	-	0.11±0.004	-
	TZ	-	0.07±0.010	-
Mirinda	SY	0.7	0.82±0.010	101.2
	TZ	1.0	1.05±0.020	98.1
	SY	-	0.09±0.010	-
	TZ	-	0.07±0.005	-
	SY	5.0	5.04±2.00	99.0
	TZ	10.0	10.3±1.70	102.1

±Shows the standard deviation with four replicates determination

Conclusion

A stable, easy to prepare, and simple voltammetric sensor was developed based on a CPE modified with ZnCrFeO₄ for simultaneous determination of SY and TZ that is preferable to other previously reported SY and TZ sensors in terms of wider dynamic range, higher selectivity, and lower detection limit. The construction of ZnCrFeO₄ modified electrode was simple and some convenient materials were needed to fabricate the sensor. Calibration curves for both SY and TZ at ZnCrFeO₄/CPE gave a pleasant linear relationship with limits of detection 2.0 nmol L⁻¹ and 10.0 nmol L⁻¹, respectively. The analytic results obtained with the ZnCrFeO₄ modified electrode shows the ability of the proposed method for simultaneous quantification of these additive dyes in food products.

Acknowledgements

The authors gratefully acknowledge support of this work by the Research Council of Payame Noor University.

References

- [1] W. Zhang, T. Liu, X. Zheng, W. Huang, C. Wan, *Colloids Surf. B*, **2009**, *74*, 28–31
- [2] K.T. Chung, C.E. Cerniglia, *Mutat. Res.*, **1992**, *277*, 201–220.
- [3] Y. Mao, Q. Fan, J. Li, L. Yu, L. Qu, *Sens. Actuators B*, **2014**, *203*, 759–765.
- [4] N.E. Llamas, M. Garrido, M.S.D. Nezio, B.S.F. Band, *Anal. Chim. Acta*, **2009**, *65*, 38–42.
- [5] S.P. Alves, D.M. Brum, E.C. Branco de Andrade, A.D. Pereira Netto, *Food Chem.*, **2008**, *107*, 489–496.
- [6] J. Wang, G. Chen, T. Zhu, S.i Gao, B. Wei, L. Bi, *Chin. Opt. Lett.*, **2009**, *7*, 1058–1060.
- [7] M. Wang, Y. Gao, Q. Sun, J. Zhao, *J. Electrochem. Soc.*, **2014**, *161*, B297–B304.
- [8] C. Yao, Q. Zeng, G.F. Goya, T. Torres, J. Liu, H. Wu, M. Ge, Y. Zeng, Y. Wang, J.Z. Jiang, *J. Phys. Chem.*, **2007**, *C111*, 12274–12278.
- [9] J. Ghodsi, A.A. Rafati, Y. Shoja, *Adv. J. Chem. A*, **2018**, *1*, 39–55.
- [10] E.A. Gomaa, M.N. Abdel Hady, M.H. Mahmoud, D.A. El Kot *Adv. J. Chem. A*, **2019**, *2*, 1–13.
- [11] S. Janitabar Darzi, N. Mohseni, *Adv. J. Chem. A*, **2019**, *2*, 165–174.
- [12] H. Noorizadeh, A. Farmany, *Adv. J. Chem. A*, **2019**, *2*, 128–135.
- [13] H. El Moussaoui, T. Mahfoud, S. Habouti, K. El Maalam, M. Ben Ali, M. Hamedoun, O. Mounkachi, R. Masrour, E.K. Hlil, A. Benyoussef, *J. Magn. Magn. Mater.*, **2016**, *405*, 181–186.
- [14] M.B. Gholivand, A. Akbari, M. Faizi, F. Jafari, *J. Electroanal. Chem.*, **2017**, *796*, 17–23.
- [15] A. Afkhami, F. Gomar, T. Madrakian, *Sens. Actuators B*, **2016**, *233*, 263–271.

- [16] M. Roushani, S.J. Hoseini, M. Azadpour, V. Heidari, M. Bahrami, M. Maddahfar, *Mater. Sci. Eng. C*, **2016**, 67, 237-246.
- [17] A.A. Ensafi, A.R. Allafchian, *Colloids Surf. B*, **2013**, 102, 687-693.
- [18] A.A. Ensafi, B. Arashpour, B. Rezaei, A.R. Allafchian, *Colloids Surf. B*, **2013**, 111, 270-276.
- [19] V. Erady, R.J. Mascarenhas, A. K. Satpati, S. Detriche, Z. Mekhalif, J. Delhalle, A. Dhason, *Mater. Sci. Eng. C*, **2017**, 76, 114-122.
- [20] A. Hamed, A.G. Fitzgerald, L. Wang, M. Gueorguieva, R. Malik, A. Melzer, *Mater. Sci. Eng. C*, **2013**, 33, 1623-1628.
- [21] W. Konicki, D. Sibera, E. Mijowska, Z. Lendzion-Bielun, U. Narkiewicz, *J. Colloid Interface Sci.*, **2013**, 398, 152-160.
- [22] I. Sharifi, H. Shokrollahi, *J. Magn. Mater.*, **2012**, 324, 2397-2403.
- [23] A.J. Bard, L.R. Faulkner, *Electrochemical Methods Fundamentals and Applications*, **1980**, Wiley, New York.
- [24] P.S. Dorraji, F. Jalali, *Food Chem.*, **2017**, 227, 73-77.
- [25] S.M. Ghoreishi, M. Behpour, M. Golestaneh, *Food Chem.*, **2012**, 132, 637-641.
- [26] T. Gan, J. Sun, S. Cao, F. Gao, Y. Zhang, Y. Yang, *Electrochim. Acta*, **2012**, 74, 151-157.
- [27] M.R. Majidi, R.F.B. Baj, A. Naseri, *Food Anal. Methods*, **2013**, 6, 1388-1397.
- [28] T. Gan, J. Sun, W. Meng, L. Song, Y. Zhang, *Food Chem.*, **2013**, 141, 3731-3737.
- [29] B. Nevado, J.R. Flores, M.J.V. Llerena, *Talanta*, **1997**, 44, 467-474.

How to cite this manuscript: Masoumeh Taei, Hossein Salavati, Masoud Fouladgar, Elmira Abbaszadeh. Simultaneous determination of sunset yellow and tartrazine in soft drinks samples using nanocrystallites of spinel ferrite- modified electrode. *Iranian Chemical Communication*, 2020, 8(1), 67-79.